J Therm Anal Calorim (2012) 109:203–215
DOI 10.1007/s10973-011-1664-9

Thermo-physical characterization of Pharmacoat® 603, Pharmacoat® 615 and Mowiol® 4-98

Giacomo Perfetti · Thibault Alphazan · W. J. Wildeboer · Gabrie M. H. Meesters

Received: 28 September 2010 / Accepted: 13 May 2011 / Published online: 2 July 2011

Abstract Hydroxypropyl methylcellulose (HPMC) and polyvinyl alcohol (PVA) are important polymers in pharmaceutical, food and other industries being largely used as encapsulation agents. The characterization of two reference grades of HPMC (Pharmacoat® 603 and Pharmacoat® 615) and one reference grade of PVA (Mowiol® 4-98), through X-ray diffraction (XRD) and thermogravimetry (TG) is described. Specific analyses were performed by means of dynamic vapour sorption analysis of water adsorption/desorption from vapours at 10, 25, 40, 55 and 70 °C. Guggenheim–Anderson–de Boer (GAB), Brunauer–Emmett–Teller (BET), Park and *n*-layer BET models were successfully used to fit the experimental data. The glass transition temperature as function of water content was measured by means of differential scanning calorimetry (DSC). The experimental data were analysed according to Linear, Gordon–Taylor, Fox and Roos equations. XRD studies revealed amorphous structure for the Pharmacoat® 603 and Pharmacoat® 615 and crystalline for Mowiol® 4-98. Single and multi-step temperature degradation point was found for Pharmacoat® 603 and Pharmacoat® 615 and Mowiol® 4-98, respectively. The water uptake is higher for Pharmacoat® 603 and Pharmacoat® 615 than Mowiol® 4-98. The influence of temperature on water uptake is opposite for the two types of polymers. GAB and *n*-layer BET were found to better model Pharmacoat® 603 and Pharmacoat® 615 and Mowiol® 4-98 data, respectively. The water makes the glass transition to decrease quite drastically. Gordon–Taylor is better fitting the experimental data both for Pharmacoat® 603 and Pharmacoat® 615 and Mowiol® 4-98.

Keywords Formulation · HPMC · PVA · Adsorption · Desorption · Thermo-physical analysis

G. Perfetti (✉) · T. Alphazan · G. M. H. Meesters
DelftChemTech DCT, NanoStructured Materials Group NSM, ChemE, Faculty of Applied Sciences, Delft University of Technology, Julianalaan 136, 2628 BL Delft, The Netherlands
e-mail: g.perfetti@tudelft.nl

W. J. Wildeboer · G. M. H. Meesters
DSM Food Specialties, P.O. Box 1, 2600 MA Delft, The Netherlands

Introduction

Film formers such as the semisynthetic derivative of cellulose hydroxypropyl methylcellulose (HPMC) and the water-soluble synthetic polymer polyvinyl alcohol (PVA) are extensively used in the coating of tablets, pellet or granule as well as a binder in the formulation of sustained release dosage forms and oral controlled drug delivery systems as a swellable and hydrophilic polymer [1–4].

Moreover, they are both appreciated for their good film-forming properties that enable the production of tough coats, protecting against degradation and moisture, preventing dust formation and breakage of the core particle, and formulation's taste masking [5], their relatively small influence of processing parameters and simple manufacturing technology [6].

The HPMC, which is a propylene glycol ether of methylcellulose, is widely used as a thickening agent, filler, anti-clumping agent and emulsifier having non-toxic property, pretty ease handling [7, 8] as well as high biodegradability, non-ionic property, and high solubility [9]. The major application of HPMC is as a carrier material in the pharmaceutical industry [8]. For the preparation of oral controlled drug delivery systems the hydrophilic material is very suitable because of its ability to let drugs slowly diffuse out of the system [10]. In food application, HPMC

has many uses: as a thickening agent, filler, dietary fibre, anti-clumping agent and emulsifier. It is prepared from cellulose, but better soluble in water than cellulose.

The substituent in its structure can be either a $–CH_3$, or a $–CH_2CH(CH_3)OH$ group, or a hydrogen atom. The methoxy ($–OCH_3$) group content, hydroxypropoxy ($–OCH_2CH(CH_3)OH$) group content and the molecular weight (MW) affect the physicochemical properties the most. Depending on the relative methoxy- and hydroxypropoxy content we can distinguish four types of polymer, namely HPMC 1828, HPMC 2208, HPMC 2906 and HPMC 2910. Variations of contents cause changes in product characteristics like, for instance, different rates of drug release in the final tablet [10].

The PVA, which is a water-soluble synthetic polymer, is another well-known suitable material for fluid bed coating. It is frequently used as thickening agent in non-food products like shampoo and latex paint. As a water-soluble film it is very suitable for envelope glue and packaging. The PVA bases its high tensile strength, flexibility, as well as high oxygen and aroma barrier to its excellent film-forming, emulsifying, and adhesive properties. It has very high grease, oil and solvent resistance together with odourless and nontoxic properties. The chemical structure of this synthetic water-soluble polymer present a molecular formula which is $(C_2H_4O)_n$. Vinyl acetate is a starting monomer unit in PVA, in which most of the acetate parts are subsequently hydrolysed to alcohol units [11]. The basic properties of PVA highly depend on the degree of hydrolysis (i.e., fully hydrolysed or partially hydrolysed grades) and viscosity [12].

HPMC and PVA are humidity (water) dependant, having various strengths of interaction with water [13]. The mechanical properties such as tensile strength, elongation and tear strength as well as the thermal properties of polymers are drastically affected by polymer's molecule–water interaction [14]. The plasticizing effect of the water enables to form stable hydrogen bonding making the polymer to produce strong compacts [15]. Moreover the analysis of effect of water on bulk polymer properties is fundamental for many activities related to coating technology [16], like the prediction of glass transition temperature, T_g [17]. The correlation between water and T_g is fundamental for the evaluation of agglomeration–stickiness ability of the coating agent, the design of drying methods as well as the selection of adequate storage conditions for the coated particles. In this context, the sorption isotherms are used as tool for measuring the water adsorption of the bulk coating agent and thus assess the relationship between water content, temperature and humidity.

The effect of temperature on the adsorption–desorption isotherm of Pharmacoat® 603 and Pharmacoat® 615 and Mowiol® 4-98 results to be crucial when establishing the storage and processing conditions. Although few authors have reported about adsorption–desorption isotherms [18, 19] and more in general about water interaction with bulk solids [20] for similar products there is no data available for these specific formulations. Moreover, the influence of temperature has not been studied yet.

This study presents a basic thermo-physical characterization of the bulk properties of two reference grades of HPMC (Pharmacoat® 603 and Pharmacoat® 615) and one reference grade of PVA (Mowiol® 4-98) together with a review of the results already presented in literature. By studying the thermo-physical characteristics of the bulk coating agents represent the first fundamental step for a deep understanding of what makes the corresponding coating better. This study is part of a larger project focussing on the characterization and modelling of coating material properties. In the first part of the study, the amorphousness/crystallinity of the bulk materials and their behaviour over a certain temperature range are analysed. The article examines the relationship between glass transition temperature, T_g, and water content of the bulk materials as a function of humidity and temperature. We will first determine the experimental glass transition temperature of the three materials as a function of water content, and then compare the experimental data with T_g models predictions. All these equations are derived considering the glass transition behaviour of amorphous solids as function of water content according to the polymer free volume theory [21]. Subsequently we measure the water up-take of the bulk materials as function of the humidity and the temperature and their interactions with water as powders. Similarly, the experimental data are compared to existing well-known models.

Materials and methods

Bulk polymers

High substituted HPMC Pharmacoat® 603 and Pharmacoat® 615 (to be referred as HPMC 603 and HPMC 615, respectively, further in this article) were supplied by Shin-Etsu Chemical Co., Japan. PVA Mowiol® 4-98 (to be referred as PVA 4-98 further in this article) was supplied by Sigma–Aldrich GmbH, Germany. All the polymers were used as received. Table 1 summarizes the characteristic properties of each polymer.

X-Ray diffraction (XRD)

HPMC 603, HPMC 615 and PVA 4-98 bulk powder XRD patterns were recorded employing a X-ray diffractometer (XRD Bruker AXS D8 Advance) Ni-filtered Cu-K_α radiation ($\lambda = 1.54178$ Å), a voltage of 20 kV, a current of

Table 1 Characteristic properties of Pharmacoat® 603 (HPMC 603), Pharmacoat® 615 (HPMC 615) and Mowiol® 4-98 (PVA 4-98)

Polymer	Grade	Degrees of substitution/% w/w		M_w	Viscosity[a]/mPa s	Mol% hydrolysis	Polymerization
		Methoxy	Hydroxypropoxyl				
Pharmacoat®	603	28.7	8.9	13000	4.5–5		
Pharmacoat®	615	28.9	8.8	65000	29–31		
Mowiol®	4–98			27000	4–4.5	98–98.8	~600

[a] 3% solution in water at 25 °C

20 mA from $2\theta = 10$ to 90 (2θ: diffraction peak angle, scan rate 20 s/step, step size: 0.01°) at room temperature. A divergence slit of 0.6 mm, anti-scatter slit of 0.6 mm and a detector slit of 0.2 mm were used.

Thermogravimetry (TG)

The TG analyses using a TG 7 (Perkin Elmer Massachusetts, USA) with a dry nitrogen purge were performed to determine either the water content of HPMC 603, HPMC 615 and PVA 4-98 at equilibrium in the desiccators with saturated salt solutions, and the thermal stability, the corresponding maximum temperature of thermal degradation and percentage of solid residue at 525 °C of the bulk polymers. Alumel (152.17 °C) and Perkalloy (594.47 °C) were used to calibrate the temperature reading and the mass measurement was calibrated using reference materials according to the manufacturer's instructions. Approximately 5–20 mg of bulk HPMC 603, HPMC 615 and PVA 4-98 stored in the saturated salts solutions ambient were placed in alumina crucibles for TG and the water content as mass loss was measured during heating from 25 to 150 °C at a heating rate of 10 °C/min followed by an isothermal step at 150 °C for 10 min. The difference between the initial and the final sample mass was used as a measure for the water content of the samples. All measurements were repeated at least twice.

Dynamic vapour sorption analysis

Moisture sorption and desorption isotherms to relate polymer water content to relative humidity (RH) were generated at 10–25–40–55–70 °C using a high performance moisture sorption analyzer Q5000 SA (TA Instruments, Zellik, Belgium). The Q5000 SA is equipped with a sensitive symmetrical thermobalance (100 mg dynamic mass range), which monitored the sample mass at a specific RH and an efficient humidity control chamber, for the accurate measurement of mass and RH. It includes a 10-position autosampler with automated pan loading, automated humidity chamber movement, and 180 mL hemispherical metal-coated quartz boats. The instrument was calibrated using sodium chloride, NaCl (25–40–60 °C: 70–77% RH) and polyvinylpyrrolidone, PVP (25 °C, 0–80% RH). An average of 5–10 mg of sample was used per each experiment. For HPMC's samples the procedure consists in 5–10% steps in RH from 0 to 85% RH following an initial drying at experimental temperature for 120 min. During drying and adsorption–desorption, equilibrium was assumed to be established when there was a mass change minor then 0.01% over a period of 2 min and a mass change minor then 0.001% over a period of 30 min, respectively. For PVA 4-98 samples, the procedure consists of 5–10% steps in RH from 0 to 85% RH following an initial drying at experimental temperature for 6 h. PVA 4-98 samples were found much more difficult to dry. During drying and adsorption–desorption, equilibrium was assumed to be established when there was a mass change minor then 0.01% over a period of 2 min and a mass change less then 0.001% over a period of 60 min, respectively. 85% RH was not included in the experiment method when testing samples at 70 °C to minimize the risk of condensation of vapour and thus failure of the test. The systems studied were considered in equilibrium since temperature and pressure were constant during measurements and the desiccators were kept hermetically closed during storage.

A number of sorption models have been reported in the literature. In this article, Guggenheim–Anderson–de Boer (GAB) [22–24], Brunauer–Emmett–Teller (BET) [25], Park [26] and n-layer BET [27] models have been used to fit the experimental data and used to generally describe the water sorption behaviour between 0.1 and 0.9 of water activity. The quality of each model has been computed in terms of root mean square error, RMSE (Eq. 1), and adjusted root mean square error, RMSEa (Eq. 2), which are calculated as follows:

$$\mathrm{RMSE} = \sqrt{\frac{\sum_{i=1}^{n} \left(w_{\mathrm{exp}} - w_{\mathrm{pred}}\right)^2}{n}} \tag{1}$$

$$\mathrm{RMSEa} = \sqrt{\frac{\sum_{i=1}^{n} \left(\frac{w_{\mathrm{exp}} - w_{\mathrm{pred}}}{w_{\mathrm{exp}}}\right)^2}{n}} (\%), \tag{2}$$

where W_{exp} and W_{pred} are, respectively, the experimental and predicted moisture content and n the number of data

points. RMSEa measure the goodness of the model as percentage (%) of error between the experimental point and the predicted one.

It as been reported that the rigidity of both GAB and BET equations, in this study used to fit HPMC 603, HPMC 615 and PVA 4-98 experimental points, prevents an adequate goodness of fit between experimental and predicted data. In the range of $a_w = 0.9–1.0$, GAB is perfectible [28] and BET seems to be unsuitable to describe the sorption isotherm of amorphous polymer involving plasticization and structural changes due the high amount of absorbed water above $a_w = 0.4$ [29]. However, Tong et al. [30] have shown that BET equation was adequate to model the water sorption of a dextran polymer (similar to HPMC) in the whole range of water activity. In Park's model, which is only used fit HPMC 603 and HPMC 615 experimental points, a different approach to moisture sorption is considered. GAB and BET models are based on a layer-by-layer condensation of water on adsorption surfaces (external as internal) whereas Park's assumes an association of three mechanisms: a specific sorption (Langmuir's law), a non specific sorption (Henry's law) and a clustering mode (water aggregation) at high water activities. Park's model is based on a five parameters equation. The Langmuir's mode is characterized by A_L, the concentration of specific sorption sites (polar groups, micro cavities or porosities) and B, the affinity constant of water for these sites. Henry's law is described by a constant K_H, and the clustering mode is based on an equilibrium constant K_a and the average number of molecules in aggregates n.

It is important to realize that GAB, BET and Park equations are empirical and based on theoretical assumptions.

Differential scanning calorimetry (DSC)

Preparation of HPMC and PVA formulations

Various water activities were considered from 0.8 to 0.03 by storing the powder formulations at eight different conditions. To obtain equilibrium moisture contents at constant temperatures standard saturated solutions of ammonium chloride (NH_4Cl), calcium nitrate tetrahydrate [$Ca(NO_3)_2{\cdot}4H_2O$], magnesium acetate [$(CH_3COO)2Mg{\cdot}4H_2O$), calcium chloride hexahydrate ($CaCl_2{\cdot}6H_2O$), lithium chloride (LiCl), silica gel and phosphorus pentoxide (P_2O_5) were used to maintain constant vapour pressure. The powder formulations were also equilibrated at fixed ambient conditions (25 °C, 40–45% RH). Glass desiccators containing the salt solutions were kept in temperature controlled rooms at 25 °C. Samples of pure HPMC 603, HPMC 615 and PVA 4-98 powders were carefully weighed using a standard analytical balance (Model 204, Mettler, Toledo, Switzerland) and placed in each desiccators with the saturated salt solutions. At least triplicate samples of each formulation were stored inside each of the seven desiccators. Values for the water activity of the salt solutions at each temperature were experimentally measured using water activity apparatus (Novasina ms1, Novasina AG, Switzerland). The mass of the samples in the desiccators was measured periodically (PG8001-S, Mettler Toledo, Switzerland). When equilibrium (two successive readings were less than 1%) was reached (less than 2 months approximately) the moisture content of the samples were determined using TG analyser, as described in Sect. 2.3. Table 2 reports the temperature and the water activity (at equilibrium) of the saturated salts solutions used in this study.

DSC studies of HPMC 603, HPMC 615 and PVA 4-98 were performed using a DSC 821e (Mettler Toledo AG, Giessen, Germany) equipped with an automatic refrigerated cooling accessory (RCS) and modulated capability, an auto-sampler tray (TSO 801R0 Mettler Toledo) and a thermal analysis data system. Nitrogen was used as the purge gas at a flow rate of 40 mL min^{-1}. The calorimeter was automatically calibrated for baseline using no pans, for cell constant using indium (melting point 156.61 °C, enthalpy of fusion 28.71 J/g), and for temperature and heat capacity using indium and tin (St). After storage at conditions listed in Table 2, the samples were accurately weighed (5–15 mg) in aluminium light pans (Al SEIKO capsule, 20 μL), covered with the lid, hermetically sealed, to prevent escape of vapourized moisture due to pressure build-up during heating cycle, and then loaded on an auto-sampler tray. The HPMC samples were heated from 25 to 225 °C, stabilized at 225 °C for 5 min, quenched to 25 °C, stabilized at 25 °C for 5 min and then reheated to 225 °C always at a rate of 10 °C/min. The PVA samples were first chilled immediately to −20 °C and held at −20 °C for 5 min. Therefore, they were up to 120 °C, stabilized at 120 °C for 5 min, quenched to −20 °C, stabilized at

Table 2 Water activity and temperatures of the saturated salts solutions used to equilibrate the formulations

Salts-equilibrium conditions	Temperature/ °C	Water activity, a_w
Ammonium chloride, NH_4Cl	25	0.791
Calcium nitrate tetrahydrate, $Ca(NO_3)_2{\cdot}4H_2O$	25	0.668
Magnesium acetate, $(CH_3COO)2Mg{\cdot}4H_2O$	25	0.58
Calcium chloride hexahydrate, $CaCl_2{\cdot}6H_2O$	25.1	0.349
Lithium chloride, LiCl	25	0.2
Silica gel	25	0.08
Phosphorus pentoxide, P_2O_5	23	0.003

−20 °C for 5 min and then reheated to 120 °C always at a rate of 10 °C/min. T_g is reported as the midpoint of the glass transition during both first and second heating. The sample pans were re-weighted after the test and the actual water content, w_c, was calculated using Eq. 1. The measurements for each formulation at each RH condition were made at least in duplicate.

Several equations describe the influence of water on glass transition. Data fittings based on the linear model, Gordon–Taylor [21], Fox [31] and Roos [32] have been carried out to predict the glass transition temperature as function of water content. In this study, a value of −135 °C was taken as glass transition of the water whilst the glass transition of the product stored in phosphorus pentoxide (P_2O_5) was taken as T_g of solid dry polymer.

Results and discussion

XRD

XRD was used to study the crystallinity–amorphous structure of the bulk powders of the HPMC 603, HPMC 615 and PVA 4-98. The three patterns are shown in Fig. 1. The HPMC 603 and HPMC 615 showed two broad specific amorphous bands in the range $2\theta = 10$–$11°$ and $2\theta = 20$–$21°$ as evident in Fig. 1a, b [33–38].

Figure 1c shows the XRD pattern of PVA 4-98 bulk solid. PVA 4-98 is a crystalline polymer and the three typical diffractions peaks at $2\theta = 19.9°$, 23° and 40.7° are evident in the plot [39, 40]. The crystalline peak of PVA 4-98 is given by the interference of the polymer chains in the direction of the hydrogen bonds [41]. More PVA chains stuck together, larger the size of the crystallite and more intense the corresponding peak.

TG

The thermal stability at a heating rate of 10 °C/min, under nitrogen, was investigated and the water content, the corresponding maximum temperature of thermal degradation and the percentage of solid residue at 525 °C calculated. In Fig. 2, the TG curves of HPMC 603, HPMC 615 and PVA 4-98 are shown. The maximum temperature of degradation, the percentage of mass loss in each stage of degradation and percentage of solid residue at 500 °C are reported in Table 3.

The obtained curves show a rapid mass loss from ambient temperature to 70 °C for HPMC 603 and HPMC 615 whereas, within the same temperature range, only a small mass loss has been detected for PVA 4-98. HPMC 603 and HPMC 615 had only one stage of degradation at

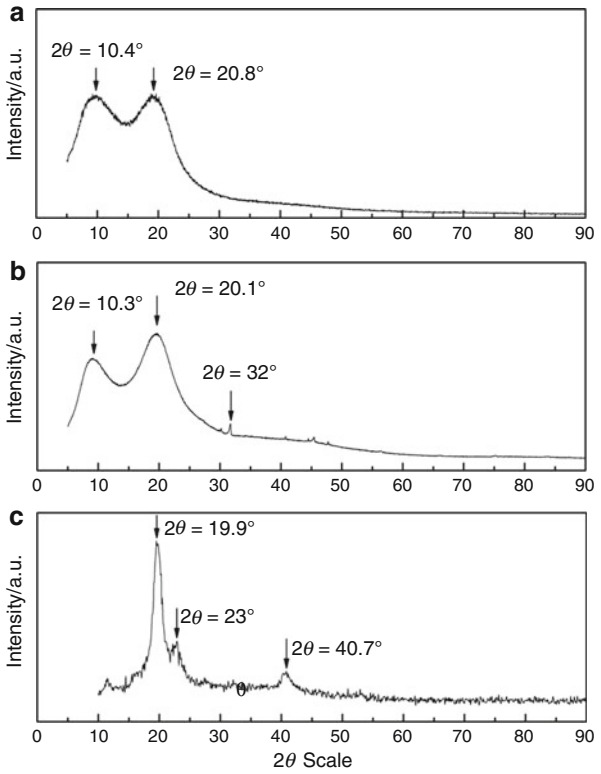

Fig. 1 XRD patterns of bulk HPMC 603 (**a**), HPMC 615 (**b**) and PVA 4-98 (**c**)

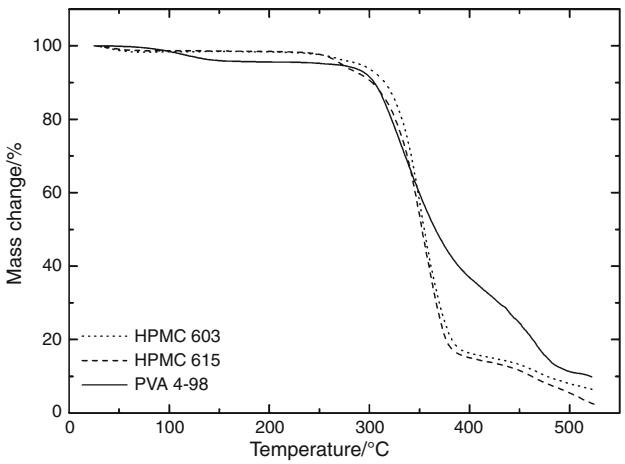

Fig. 2 TG curves between 25 and 525 °C for the polymer HPMC 603 (*dotted line*), HPMC 615 (*dashed line*) and PVA 4-98 (*solid line*) at a heating rate of 10 °C min^{-1}

$T_{deg} = 376.5$ and 382.8 °C, respectively, [42] measured in correspondence of 80% mass loss indicating that HPMC 603 is less thermally stable than HPMC 615. The quick loss in mass was attributed to evaporation of not-bounded moisture present on the surface of the solids.

The PVA 4-98 had two main stages of degradation: the first one with T_{deg} at 396 and 484 °C corresponding to 62.04 and 86.65% of mass loss, respectively. Such

Table 3 TG parameters for HPMC 603, HPMC 615 and PVA 4-98

Polymer	Mass loss/%		Temperatures of degradation/°C	Residual mass at 500 °C/%
	25–70 °C	25–150 °C		
HPMC 603	1.29	1.41	280–300	5.49
HPMC 615	1.54	1.73	280–300	8.02
PVA 4-98	0.41	4.03	280–300	11.29

degradations steps correspond to the degradation of vinyl acetate and vinylpyrrolidone, respectively, suffering the PVA a deacetylation in the temperature range 160–400 °C [43].

Dynamic vapour sorption analysis

The objective of this part of the study is to measure the tendency of HPMC 603, HPMC 615 and PVA 4-98 to uptake–release water from the environment over their usual coating–drying–storage temperature range. Water sorption isotherms relate the water content contained in the formulations to the RH of the environment and thus to the water activity of such formulations. In polymers, water can be both adsorbed on the surface and absorbed in the bulk. HPMC's and PVA 4-98 have a different degree of crystallinity, and the sorption behaviour of crystalline regions is totally different from amorphous regions. Amorphous region will tend to be hydrated from the solid to rubbery to liquid state, taking up the largest quantity of water during the sorption process, whereas crystalline regions will only change from the solid to liquid state. Thus, as a matter of fact, values as W_m should be corrected to take into account the amorphous content. In our case, XRD experiments on the HPMC 603, HPMC 615 and PVA 4-98 have shown the total amorphousness of HPMC's and three crystalline peaks for PVA 4-98. Experimental equilibrium data for the sorption isotherm of HPMC 603, HPMC 615 and PVA 4-98, at room temperature (25 °C) over a range of water activity of 0–0.85 is shown in Fig. 3. GAB, BET and Park models were used to fit the obtained experimental data for HPMC's samples whilst GAB, BET and *n*-layer BET in case of PVA 4-98 samples.

Figure 3 shows the moisture sorption isotherms for HPMC 603, HPMC 615 and PVA 4-98 at room temperature, 25 °C (Fig. 3a), and the fit of GAB, BET and Park equations for HPMC 603 and HPMC 615, and the fit of GAB (dashed line), BET (dotted line) and *n*-layer BET (solid line) equations for PVA 4-98 (Fig. 3b). All isotherms show an increase in equilibrium moisture content with increasing water activity. Equilibrium moisture for HPMC powders increased slowly (and linearly) between 0 and 0.45 a_w; from this value up, higher water activities implied a substantial water gain in the powders achieving 12.4 and 13.2% db at 85% RH for HPMC 603 and HPMC 615,

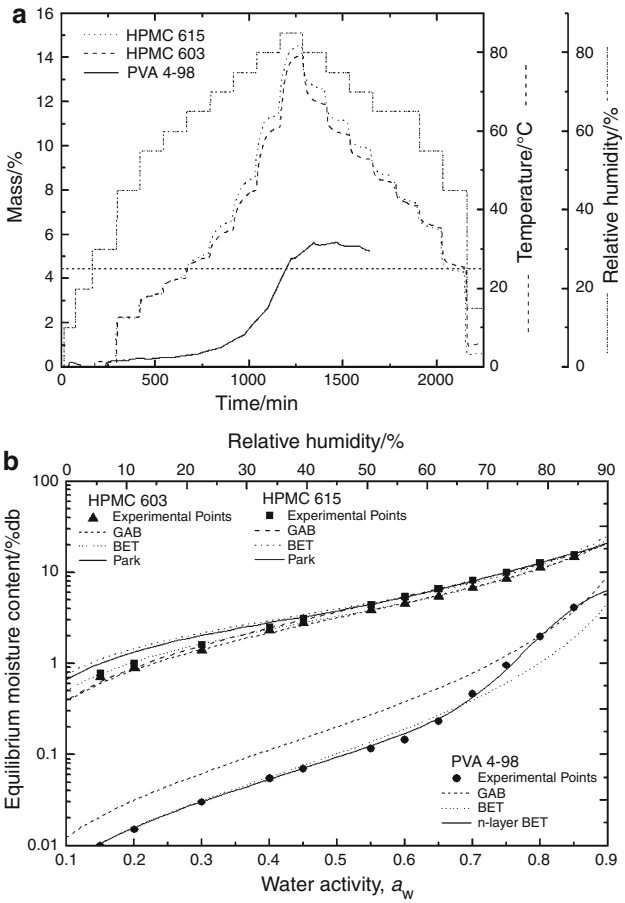

Fig. 3 Moisture sorption isotherms for HPMC 603, HPMC 615 and PVA 4-98 at room temperature, 25 °C (**a**) and the fit of GAB (*dashed line*), BET (*dotted line*) and Park (*solid line*) equations for HPMC 603 and HPMC 615, and the fit of GAB (*dashed line*), BET (*dotted line*) and *n*-layer BET (*solid line*) equations for PVA 4-98 (**b**)

respectively, and the latter showing a bigger capacity for water adsorption. PVA 4-98 does not absorb moisture until 50–55% RH is reached afterwards a drastic increase in water gain is observed which is typical of crystalline compounds. At low temperatures no physical or chemical changes are produced, and the energy levels reached are insufficient to allow great water mobility determining the hydrophobic character of the product. The diffusion rate of the water through HPMC 603 and HPMC 615 is much higher compared to the one from PVA 4-98 resulting in longer time for the latter to reach the equilibrium at each RH

step (Fig. 3a). Above 45% RH the water uptake per each RH step (5% constant) increases drastically with increasing RH (Fig. 3a). This behaviour is not present during desorption where per each 5% RH step the same amount of water is released. This is due to the existence of two simultaneous phenomena during adsorption:diffusion of water through the material and chemical bonding water-material into the structure. The water, in fact, which has bonded in the structure, remains in the material during desorption leading to a water content at the end of desorption (0% RH) higher than at beginning of the adsorption (0% RH). As we can see in Fig. 3b, HPMC exhibits at 25 °C a typical S-shape isotherm known as type II isotherm in Brunauer classification [27]. Amongst the three pure products, HPMC 615 first and HPMC 603 s showed the highest water affinity and water binding capacity due to the large amount of hydrophilic groups present in their structure. For HPMC's materials in the first segment at low RH an S-like shaped sorption isotherm curves is obtained, whereas no relevant absorption can be detected for PVA 4-98.

Figure 4a, b and c shows the temperature (10–25–40–55–70 °C) effect on the sorption isotherms of HPMC 603, HPMC 615 and PVA 4-98, respectively. All isotherms show an increase in equilibrium moisture content with increasing water activity, at each temperature. For HPMC 603 and HPMC 615 an increase in temperature causes a decrease in water activity. This might be due to physico-chemical changes that result in a loss of water sorption active points in the products. It is remarkable that differences are more pronounced for HPMC 615 than for HPMC 603. For each temperature, the HPMC 615 isotherms are always above the isotherms of the HPMC 603. In both cases at low water activity practically no effect of temperature on the sorption isotherm is observed. The dependence with temperature is clearer at higher water activity and when a wide range of temperatures is studied.

For PVA 4-98 the effect of temperature is opposite. Like for most solutions and food products [44] an increase in the temperature leads to an increase in the water activity. This happens in the all range of temperature (10–70 °C) and water activity.

The experimental adsorption data obtained as function of temperature were fitted using the model described above and the resulting calculated coefficients are listed in Table 4. BET, GAB and Park prediction curves are similar in the upper range of a_w (between 0.5 and 0.9) but tend to separate for low water activities. For RH below 40% especially BET and Park models do not gives reliable results with the increase of the equilibrium temperature. However, at 10 °C the K value of the GAB equation is closed to unity, meaning that BET seams to be the best model for low temperature. But the increase of temperature makes C_{BET} to decrease consistently with its definition

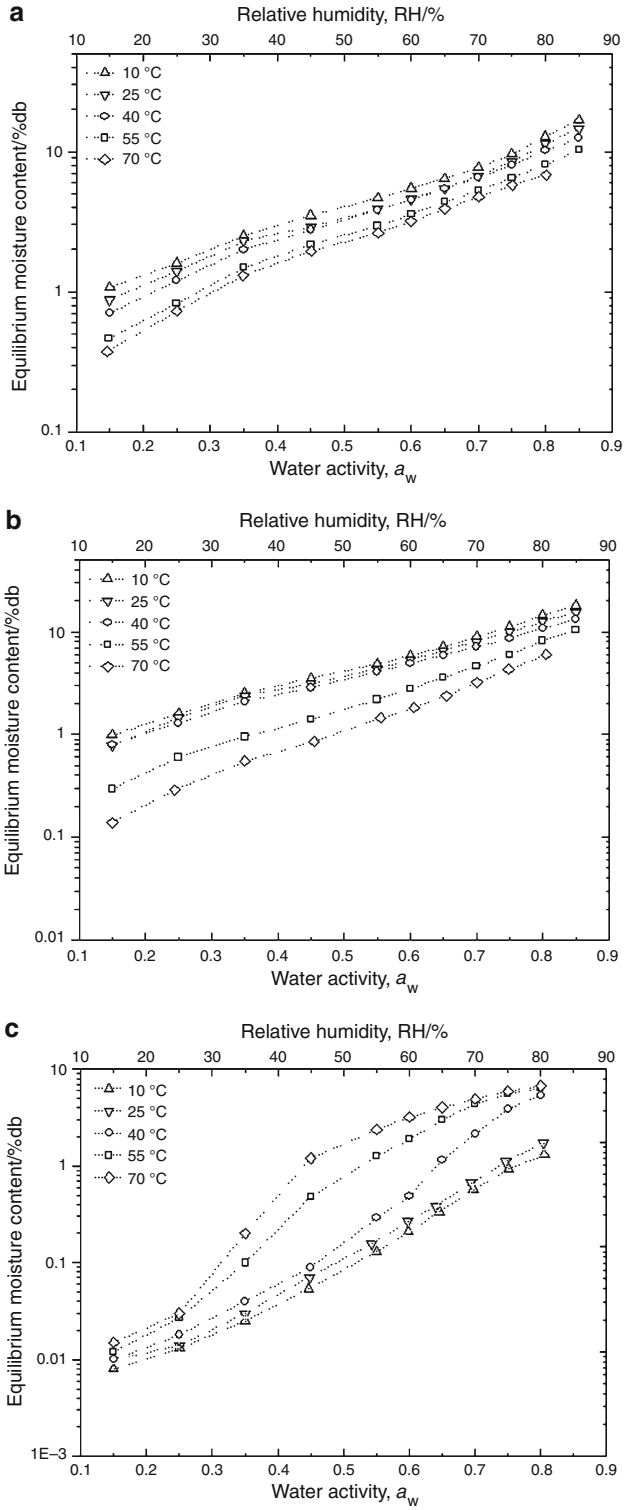

Fig. 4 Moisture sorption isotherms for HPMC 603 (**a**), HPMC 615 (**b**) and PVA 4-98 (**c**) at 10 °C (*triangle*), 25 °C (*inverted triangle*), 40 °C (*open circle*), 55 °C (*open square*) and 70 °C (*open diamond*)

[27], and, parallel, to only slightly decrease K making the GAB model more accurate. Nonetheless, the quality of the fitting at low water activities decreases at high equilibrium

temperatures as demonstrated by increasing in RMSEa. Overall, for HPMC's the predicted data are generally better fitted with the GAB model as shown by the lower RMSE and RMSEa values in Table 4. The main difference between the two grades of HPMC is the quantity of water adsorbed. Table 4 shows that HPMC 615 absorbs, on average, two time more water than HPMC 603 (6 vs. 3%) in agreement with the values found by Tong et al. [30]. W_m, which can be considered as the amount of water required to saturate the accessible biding sites both on the surface and in the bulk material [30], is not constant and a clear tendency could not be found. Moreover, Table 4 shows that HPMC 615 adsorbs more water than HPMC 603 as well as the higher heat of adsorption of water, C, for HPMC 603 compared to HPMC 615 grade. Then, consistent with the article of Timmermann [45], the calculated BET and GAB constants presented before follow the inequalities $W_{m(BET)} < W_{m(GAB)}$ and $C_{BET} > C_{GAB}$. Timmermann has also shown that only the GAB constants have to be taken as the representative parameters of the multilayer sorption.

Park's model has proved to be visually as good as BET and GAB but fitting problems still remain. In fact, the A_L and B values obtained, 0.001 and 50, respectively, are not in agreement with their physical meaning apparently. Being A_L the Y-intercept in the linear extrapolation used, one explanation is that the materials show a very low water uptake between $a_w = 0.1$ and 0.3 (range of a_w used for this linear extrapolation) or that the initial curvature of the isotherm is not concave but convex. This leads to the rigidity of each model which, of course, has to be improved for low water activities. Moreover, this very low value of A_L (closed to 0 g water/g of cellulose) which should represent the amount of hydrophilic groups is not in accordance with the theoretical amount of 0.33 g water/g of cellulose calculated for three molecules of water per—$C_6H_{10}O_5$—unit. This could be due to the substitution of hydroxyls by methoxy groups considered as hydrophobic (28–30% of methoxy groups in the tested HPMC). The strongly bonded water molecules could remain in the sample even after drying, leading to an overestimation of the dry mass of the sample and a diminution of the free sorption sites [46]. Moreover, the strong hydrogen bonds inside the structure could also prevent water molecule to binding easily.

The variation of the coefficients K_H, K_a and n with the increasing temperature is logical. At higher temperatures, it is harder for water molecules to adsorb on the surface so K_H decreases, as well as K_a and n because aggregates are formed slower than for lower temperatures and are made of fewer molecules. Overall, if we neglect the very low a_w, the fitting remains interesting with a RMSE lower than the BET one, making this model really promising to describe sorption phenomena of cellulose-based material.

For PVA 4-98 both BET and GAB models, which have previously been applied successfully [47, 48] although for different experimental conditions, have shown some inconsistencies in predicting the experimental data. Indeed, for each equilibrium temperature, high RMSE and RMSEa values are observed in Table 4 due to a plateau which appears for water activities above 0.75. This behaviour is typical of types IV and V isotherms described by the n-layer BET equation of Brunauer [25]. In this equation, originally used for gas adsorption on solids and based on the classical BET equation, two new parameters are added. A parameter n related to a limit to the maximum number of layers that can be adsorbed is taken into account as well as g, a parameter linked to the energy balance between the n-layer binding energy and heat of evaporation [49].

As first attempt of using this model for polymeric materials a fixed value for g was chosen to avoid possible variation with the temperature. Repeated simulations have given a default average value of 540, which was used as reference, and a maximum number of 13 layers, n, used as initial condition for this study. With these values, this expanded BET equation showed a better goodness of fit, reached with RMSE between 0.02 and 0.3 as shown in Table 4 and Fig. 5.

The calculated C values follow the same tendency as for HPMC whilst the monolayer volume, W_m, increases from 0.15 to 1.58%. It is consistent with the water uptake which increases if the equilibrium temperature increases. We suppose that it is due to the structural change of the polymer. The glass transition of this grade of PVA is around 45–50 °C, and the monolayer volume, quite similar until 25 °C, changes suddenly at 40 °C and after. In the rubbery state, the lowest entanglement of the polymer chains may make binding sites more accessible and facilitate water adsorption on these binding but usually not "active binding sites" (if the temperature is lower than the glass transition). The simulated number of water layers decreases from 13 to 6, but calculations with the maximum water uptake and W_m give fewer layers than the previous ones (from 13 to 4 layers). Finally, simulated values tend to give higher numbers of layer for high temperatures.

Overall, these results indicate that, over the range of temperatures 10–70 °C, the HPMC and PVA products studied exhibits completely different hygroscopicities and behaviours with water, which means that from a practical point of view such products need to be stored, preserved and handled carefully not in the same way but with appropriate RH and temperature. Moreover, their propensity to adsorb less or more water might be also used to explain some typical behaviour in coating–drying processes.

DSC

DSC of row HPMC 603, HPMC 615 and PVA 4-98 powders equilibrated at different RH ambient has been

Table 4 Parameters values derived from water sorption data at considered temperatures from the GAB, BET, Park and *n*-layer BET equations for HPMC 603, HPMC 615 and PVA 4-98

	HPMC 603					HPMC 615					PVA 4-98				
	10 °C	25 °C	40 °C	55 °C	70 °C	10 °C	25 °C	40 °C	55 °C	70 °C	10 °C	25 °C	40 °C	55 °C	70 °C
GAB model															
C_{GAB}	2.67	1.6	1.54	1.43	0.88	0.7	0.62	0.79	0.17	0.15	0.02	0.0008	0.005	0.009	0.015
W_m/g/100 g	2.76	2.73	3.13	2.45	3.2	6.08	6.39	5.25	8.79	5.33	2.87	119.7	65.56	63.55	144.5
K	1	0.98	0.93	0.94	0.86	0.9	0.87	0.86	0.86	0.92	1	1	0.97	0.97	0.73
RMSE	0.15	0.16	0.13	0.1	0.08	0.19	0.11	0.08	0.22	0.02	0.05	0.23	0.55	0.25	0.41
RMSEa/%	2	2	6	5	6	10	7	7	14	3	80	265	905	20	850
BET model															
C_{BET}	2.89	2.08	5.2	2.78	2.43	2.68	3.22	5.04	0.94	0.38	0.0004	0.00087	0.05	0.069	0.003
W_m	2.69	2.44	2.03	1.73	1.59	3	2.61	2.18	1.94	2.02	104.5	138.7	5.9	8.52	144.4
RMSE	0.15	0.2	0.33	0.26	0.2	0.41	0.43	0.44	0.32	0.05	0.8	0.79	0.55	0.26	1.17
RMSEa/%	1	4	11	10	19	7	15	18	13	3	121	112	899	20	242
PARK model															
A_L	0.001	0.001	0.001	0.001	0.001	0.001	0.001	0.001	0	0.001	–	–	–	–	–
B	50	50	50	50	50	50	50	50	50	50	–	–	–	–	–
K_H	0.082	0.069	0.067	0.045	0.016	0.083	0.067	0.062	0.02	0.032	–	–	–	–	–
K_a	0.41	0.39	0.23	0.16	0.17	0.39	0.28	0.2	0.2	0.11	–	–	–	–	–
N	8.6	8.7	7.2	5.7	5.8	7.5	6	5.5	5.2	4.3	–	–	–	–	–
RMSE	0.18	0.22	0.17	0.17	0.2	0.35	0.22	0.12	0.21	0.06	–	–	–	–	–
RMSEa/%	6	8	6	10	11	10	10	6	11	25	–	–	–	–	–
n-layer BET															
C	–	–	–	–	–	–	–	–	–	–	0.19	0.06	0.04	0.05	0.04
N	–	–	–	–	–	–	–	–	–	–	13	13	12	8	6
V_m	–	–	–	–	–	–	–	–	–	–	0.15	0.31	1.29	1.23	1.58
G	–	–	–	–	–	–	–	–	–	–	540	540	540	540	540
RMSE	–	–	–	–	–	–	–	–	–	–	0.02	0.09	0.08	0.12	0.27
RMSEa/%	–	–	–	–	–	–	–	–	–	–	18	37	12	12	21

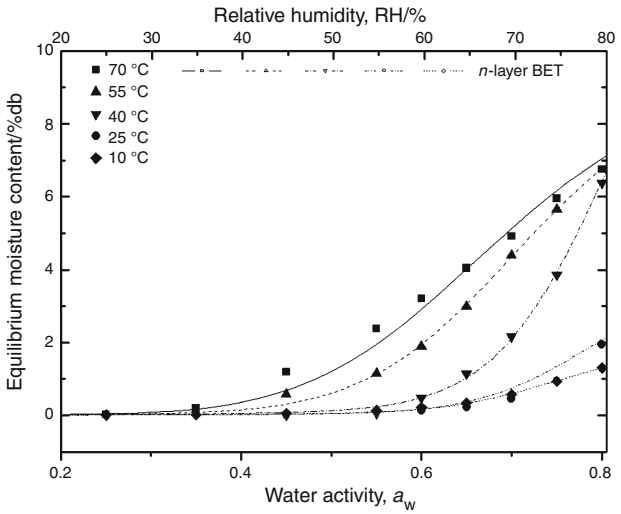

Fig. 5 Moisture sorption isotherms for PVA 4-98 at 10 °C (*filled diamond*), 25 °C (*filled circle*), 40 °C (*inverted filled triangle*), 55 °C (*filled triangle*), and 70 °C (*filled square*)

performed to measure the effect of moisture content and molecular mass on glass transition temperature.

Water content effect

The ability of water to drastically modify the behaviour of amorphous polymer has been studied for many years. Its plasticizing effect induces a physical transition from a brittle to a ductile state due to the increased mobility of polymer chains, the sliding of big polymer chains and the movement ability of incorporated short chains and extremities of such chains. Moreover, water attenuates the development of internal stresses avoiding the creation and growing of cracks. The knowledge of the influence of water on this transition, reflected by the glass transition temperature is a key factor to control mechanical properties of the material or diffusion of solute in the polymer matrix.

Figure 6 shows actual T_g versus water content data for HPMC 603 (a), 615 (b) and PVA 4-98 (c). As water content increased, the T_g of HPMC 603, HPMC 615 and PVA 4-98 decreased, indicating that water acts as plasticizer for all three polymers. The dry HPMC 603 T_g was found to be 125.5 °C, about 25 °C lower than HPMC 615 [10–14, 50, 51]. In general the same amount of water had a greater plasticizing effect on HPMC 603 than not HPMC 615 being the decrease of HPMC 603 T_g greater than that of HPMC 615. PVA 4-98 presents a dry T_g much lower, in the order of 50 °C [52, 53].

The circles, diamond, squared and triangle curves in Fig. 5 represent the fits of the experimental data to the Linear, Gordon–Taylor, Fox and Roos equations, respectively. For each material, the models have been plotted on

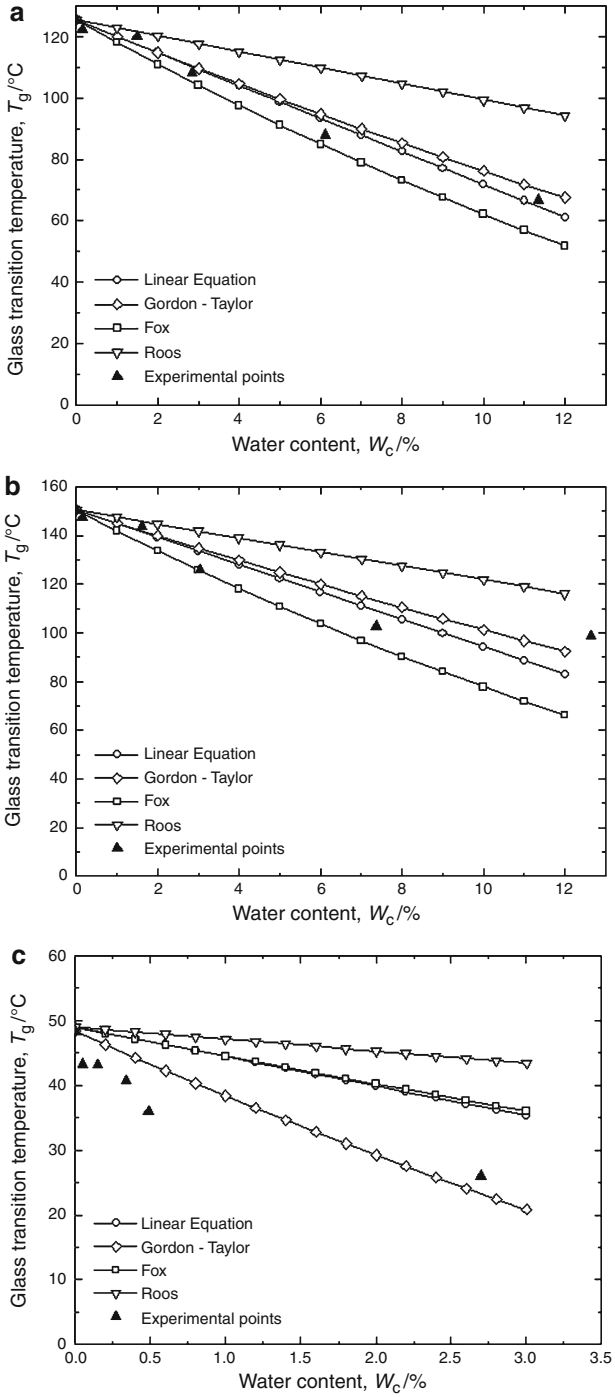

Fig. 6 Water content effect on glass transition temperature of HPMC 603 (**a**), HPMC 615 (**b**) and PVA 4-98 (**c**) and the fit of linear (*open circle*), Gordon–Taylor (*open diamond*), Fox (*open square*), Roos (*inverted open triangle*) equations and experimental points (*filled triangle*)

the range of water uptake determined in the adsorption isotherm part and characteristic of typical coating processes for these reference formulations. It means that in average, for HPMC's moisture content is varying from 0 to

Table 5 Computed values of linear, Gordon–Taylor, Fox and Roos parameters and RMSE (Eq. 2) obtained from the analysis of the relationship between water content and glass transition temperature of HPMC 603, HPMC 615 and PVA 4-98

Polymer	Linear			Gordon–Taylor			Fox			Roos		
	T_g1/K	T_g2/K	RMSE	k	T_g	RMSE	T_g1/K	T_g2/K	RMSE	T_g1/K	T_g2/K	RMSE
HPMC 603	398.65	138	7.73	2.09	125.5	6.67	398.65	138	11.11	398.65	138	13.70
HPMC 615	423.52	138	8.96	1.88	150.37	7.05	423.52	138	16.59	423.52	138	14.04
PVA 4-98	322.15	135	7.47	5.7	48.35	4.36	322	135	7.54	322.15	135	9.94

15 and from 0 to 9%wt for PVA 4-98. In Table 5, all the model's parameters obtained by the fittings are presented. In case of HPMC's, the observed depression of T_g by an increase in water content was well described by all the equation except Roos one, suggesting that the mixing behaviour of water with HPMC might be considered ideal. In particular for both HPMC 603 and HPMC 615 the fit of the simplified Gordon–Taylor and the Linear model plots to the experimental T_g data are pretty good over the entire range of water contents normally encountered during coating process. Between the two Gordon–Taylor seems to be the best as also demonstrated by the lower values of RMSE in Table 5. For HPMC 603 the Gordon–Taylor fit is particularly close at low water contents, whereas at higher values of water content a lower T_g than measured is predicted. For HPMC 615 the Gordon–Taylor fit gives T_g values lower than measured whilst at 12% water content a higher T_g than measured is predicted. The values obtained from Fox fitting result to be always slightly lower than experimental ones, whereas Roos model was found to be totally un-reliable predicting T_g higher than 30 °C even. For PVA, the models cannot predict very well the experimental data. The latter's are all higher than the ones predicted by the models all over the water content range. Amongst the others Gordon–Taylor seems once more the closest one to the experimental data. This result is confirmed by the RMSE comparison. The knowledge of water content effect results extremely important for our final purpose. The decrease–increase of T_g as function of water content can determine serious problems (i.e., stickiness and agglomeration) whilst spraying the coating agent. Moreover, it represents a relevant interaction which needs to be taken into account during storage of both bulk materials and final coated pallets. High RH environments could lead to a drastic decrease of T_g with a corresponding decrease of the maximum functional temperature of the compound.

Conclusions

Two grades of HPMC and one grade of PVA were extensively characterized. Their bulk crystallinity–amorphousness was assessed by means of XRD whereas their stability against temperature was detected using TG. The ability to uptake water and the glass transition temperature as function of water content were measured by dynamic vapour sorption analysis and DSC, respectively. The HPMC's have been found to have amorphous structure as no crystalline peaks could be detected in the X-ray paths. On the contrary, PVA was found to be crystalline in agreement with similar past studies. The temperature effect on these bulk polymers was similar for all the analysed polymers although PVA presented a multi-step temperature degradation point differently from the single-step one from HPMC's. The water uptake ability was higher for HPMC's. PVA does not adsorb any water at low RH whilst quite consistent amount of water at high RH. GAB, BET, Park and n-layer BET models were successfully used to fit the experimental data. Overall GAB and n-layer BET were found to better model HPMC's and PVA's data, respectively.

The glass transition temperature of HPMC's and PVA was measured as function of water content in the structure. The water content was found to drastically influence the glass transition temperature making it to decrease as results of its plasticizing effect on molecules. The experimental data were fitted using the Linear, Gordon–Taylor, Fox and Roos equations. Gordon–Taylor and, in some cases Fox, were the only ones able to successfully fit the data.

References

1. Alderman DA. A review of cellulose ethers in hydrophilic matrices for oral controlled-release dosage forms. Int J Pharm Tech Prod Mfr. 1984;5(3):1–9.
2. Ford JL, Rubinstein MH, Hoagen JE. Formulation of sustained release promethazine hydrochloride tablets using hydroxypropylmethylcellulose matrices. Int J Pharm. 1985;24:327–38.
3. Dansereau R, Brock M, Redman-Furey N. The solubilization of drug and excipient into a hydroxypropylmethylcellulose (HPMC)-based film coating as a function for the coating parameters in a 24″ Accela-Cota®. Drug Dev Ind Pharm. 1993;19:809–26.

4. Heinamaki J, Ruotsalinen M, Lehtola VM, Antikainen O, Yliruusi J. Optimization of aqueous-based film coating of tablets performed by a side-vented pan-coating system. Pharm Dev Technol. 1997;2:357–64.
5. Poter SC. Controlled-release film coating based on ethylcellulose. Drug Dev Ind Pharm. 1989;15:1495–521.
6. Shah NH, Railkar AS, Phauapradit W, Zeng F, Chen A, Infeld MH, Malick AW. Effect of processing techniques in controlling the release rate and mechanical strength of hydroxypropylmethylcellulose based hydrogel matrices. Eur J Pharm Biopharm. 1996; 42:183–7.
7. Freely LC, Davis SS. Influence of polymeric excipients on drug release from hydroxypropylmethylcellulose matrices. Int J Pharm. 1988;44:131–9.
8. Chatlapalli R, Rohera BD. Study of effect of excipient source variation on rheological behavior of diltiazem HCl-HPMC wet masses using a mixer torque rheometer. Int J Pharm. 2002; 238(1–2):139–51.
9. Sakata Y, Shiraishi S, Otsuka M. A novel white film for pharmaceutical coating formed by interaction of calcium lactate pentahydrate with hydroxypropyl methylcellulose. Int J Pharm. 2006;317:120–6.
10. Siepmann J, Peppas NA. Modeling of drug release from delivery systems based on hydroxypropyl methylcellulose (HPMC). Adv Drug Deliv Rev. 2001;48:139–57.
11. Dale DA, Gaertner AL, Park G, Becker NT (1999) Coated enzyme-containing granule. US Patent 5,879,920, USA. Date issued: March 9, 1999 Filed: December 22, 1995.
12. Soltani S, Asempour H, Jamshidi H. Investigation of reaction conditions for preparation of medium molecular weight poly (vinyl alcohol) as emulsifier. Iran Polym J. 2007;16(7):439–47.
13. Hatakeyama H, Hatakeyama T. Interaction between water and hydrophilic polymers. Thermochim Acta. 1998;308:3–22.
14. Nokhodchi A, Ford JL, Rowe PH, Rubinstein MH. The influence of moisture content on the consolidation properties of hydroxypropylmethylcellulose K4M (HPMC 2208). J Pharm Pharmacol. 1996;48:1116–21.
15. Ford JL. Thermal analysis of hydroxypropylmethylcellulose and methylcellulose: powders, gels and matrix tablets. Int J Pharm. 1999;179:209–28.
16. Bajdik J, Pintye-Hódi K, Regdon G, Fazekas P, Szabó-Révész P, Erős I. The effect of storage on the behaviour of Eudragit NE free film. J Therm Anal Calorim. 2006;73(2):607–13.
17. Schneider HA. The meaning of the glass temperature of random copolymers and miscible polymer blends. J Therm Anal Calorim. 1999;56(3):983–9.
18. Villalobos R, Hernandez-Munoz P, Chiralt A. Effect of surfactants on water sorption and barrier properties of hydroxypropyl methylcellulose films. Food Hydrocolloids. 2006;20:502–9.
19. Nokhodchi A, Ford JL, Rubinstein MH. Studies on the interaction between water and (hydroxypropyl)methylcellulose. J Pharm Sci. 1997;86(5):608–15.
20. Lue SJ, Shieh S. Modeling water states in polyvinyl alcohol-fumed silica nano-composites. Polym J. 2009;50:654–61.
21. Gordon M, Taylor JS. Ideal co-polymers and the second order transitions of synthetic rubbers. 1. Non crystalline co-polymers. J Appl Chem. 1952;2:493–500.
22. Guggenheim EA. Application of statistical mechanics. Oxford.: Clarendon Press; 1966.
23. Anderson RB. Modification of the Brunauer, Emmett and Teller equation. J Am Chem Soc. 1946;68:686.
24. de Boer JH. The dynamical character of adsorption. Oxford: Clarendon Press; 1953. p. 57.
25. Brunauer S, Emmett PH, Teller E. Adsorption of gases in multimolecular layers. J Am Chem Soc. 1938;60(2):309–19.
26. Park GS. Transport principles-solution, diffusion and permeation in polymer membranes. In: Bungary PM, et al., editors. Synthetic membranes: science engineering and applications. Holland: Reidel Publishing; 1986. p. 57–107.
27. Brunauer S, Deming LS, Deming WE, Teller E. A theory of Van der Waals adsorption of gases. J Am Chem Soc. 1940;62:1723–32.
28. Blahovec J, Yanniotis S. GAB generalized equation for sorption phenomena. Food Bioprocess Technol. 2008;1:82–90.
29. Labuza TP. Sorption phenomena in foods. Food Technol. 1968; 22:263–72.
30. Tong HHY, Wong SYS, Law MWL, Chu KKW, Chow AHL. Anti-hygroscopic effect of dextrans in herbal formulations. Int J Pharm. 2008;363:99–105.
31. Fox TG, Flory PJ. Second order transition temperatures and related properties of polystyrene. 1. Influence of molecular weight. J Appl Phys. 1950;21:581–91.
32. Roos Y. Phase transitions in foods. San Diego: Academic Press Inc; 1995. p. 366.
33. Dorozhkin SV. Is there a chemical interaction between calcium phosphates and hydroxypropylmethylcellulose (HPMC) in organic/inorganic composites? J Biomed Mater Res. 2001;54(2):247–55.
34. Cilurzo F, Minghetti P, Casiraghi A, Montanari L. Characterization of nifedipine solid dispersions. Int J Pharm. 2002;242(1–2):313–7.
35. Vamshi Vishnu Y, Chandrasekhar K, Ramesh G, Madhusudan Rao Y. Development of mucoadhesive patches for buccal administration of carvedilol. Curr Drug Deliv. 2007;4:27–39.
36. Bhise SB, Rajkumar M. Effect of HPMC on solubility and dissolution of carbamazepine form III in simulated gastrointestinal fluids. Asian J Pharm. 2008;2(1):38–42.
37. Rajarajan S, Baby B, Ramesh K, Singh D. Preparation and evaluation of ternary mixing itraconazole solid dispersions by spray drying method. J Pharm Sci Res. 2009;1(1):22–5.
38. Ma X-D, Qian X-F, Yin J, Zhu Z-K. Preparation and characterization of polyvinyl alcohol–selenide nanocomposites at room temperature. J Mater Chem. 2002;12:663–6.
39. Garcıa-Cerda LA, Escareno-Castro MU, Salazar-Zertuche M. Preparation and characterization of polyvinyl alcohol–cobalt ferrite nanocomposites. J Non Cryst Solids. 2007;353:808–10.
40. Hong PD, Chen JH, Wu HL. Solvent effect on structural change of poly(vinyl alcohol) physical gels. J Appl Polym Sci. 1998;69: 477–2486.
41. Zohuriaan MJ, Shokrolahi F. Thermal studies on natural and modified gums. Polym Test. 2004;23:575–9.
42. Zaccaron CM, Oliveira RVB, Guiotoku M, Pires ATN, Soldi V. Blends of hydroxypropyl methylcellulose and poly(1-vinylpyrrolidone-co-vinyl acetate): miscibility and thermal stability. Polym Degrad Stabil. 2005;90:21–7.
43. McNeill IC, Ahmed S, Memetea L. Thermal degradation of vinyl acetate-methacrylic acid copolymer and the homopolymers. II. Thermal analysis studies. Polym Degrad Stabil. 1995;48(1):89–97.
44. Alhamdan AM, Hassan BH. Water sorption isotherms of date pastes as influenced by date cultivar and storage temperature. J Food Eng. 1999;39:301–6.
45. Timmermann EO. Multilayer sorption parameters: BET or GAB values? Colloids Surf A Physicochem Eng Aspect. 2003;220:235–60.
46. Bessadok A, Langevin D, Gouanvé F, Chappey C, Roudesli S, Marais S. Study of water sorption on modified Agave fibres. Carbohydr Polym. 2009;76:74–85.
47. Lai MC, Hageman MJ, Schowen RL, Borchardt RT, Topp EM. Chemical stability of peptides in polymers. 1. Effect of water on peptide deamidation in poly(vinyl alcohol) and poly(vinyl pyrrolidone) matrixes. J Pharm Sci. 1999;88(10):1074–80.
48. Srinivasa PC, Ramesh MN, Kumar KR, Tharanathan RN. Properties and sorption studies of chitosan–polyvinyl alcohol blend films. Carbohydr Polym. 2003;53:431–8.

49. Do DD. Adsorption analyses equilibria and kinetics, vol 2. London: Imperial College Press; 1998. p. 94–99.
50. Alencar JS, Pietri S, Culcasi M, Orneto C, Piccerelle P, Reynier JP, Portugal H, Nicolay A, Kaloustian J. Interactions and antioxidant stability of sesamol in dry-emulsions. J Therm Anal Calorim. 2009;98(1):133–43.
51. Lee S, Nam K, Kim MS, Jun SW, Park J-S, Woo JS, Hwang S-J. Preparation and characterization of solid dispersions of itraconazole by using aerosol solvent extraction system for improvement in drug solubility and bioavailability. Arch Pharm Res. 2005;28(7):866–74.
52. Aoi K, Takasu A, Tsuchiya M, Okada M. Miscibility of chitin-graft-poly(2-ethyl-2-oxazoline) with poly(vinyl alcohol). Macromol Chem Phys. 1998;199:2805–11.
53. Chuang W-Y, Young T-H, Yao C-H, Chiu W-Y. Properties of the poly(vinyl alcohol)/chitosan blend and its effect on the culture of fibroblast in vitro. Biomaterial. 1999;20:1479–87.